



HAL
open science

A model for full-field optical coherence tomography in scattering media

Ugo Tricoli, Rémi Carminati

► **To cite this version:**

Ugo Tricoli, Rémi Carminati. A model for full-field optical coherence tomography in scattering media. SPIE Photonics Europe: Biomedical Spectroscopy, Microscopy, and Imaging, Apr 2020, Virtual, United States. pp.21, 10.1117/12.2555732 . hal-03206902

HAL Id: hal-03206902

<https://hal.science/hal-03206902>

Submitted on 23 Apr 2021

HAL is a multi-disciplinary open access archive for the deposit and dissemination of scientific research documents, whether they are published or not. The documents may come from teaching and research institutions in France or abroad, or from public or private research centers.

L'archive ouverte pluridisciplinaire **HAL**, est destinée au dépôt et à la diffusion de documents scientifiques de niveau recherche, publiés ou non, émanant des établissements d'enseignement et de recherche français ou étrangers, des laboratoires publics ou privés.

A model for full-field optical coherence tomography in scattering media

Ugo Tricoli^{1,2*} and Rémi Carminati¹

¹*Institut Langevin, ESPCI Paris, CNRS, PSL University, 1 rue Jussieu, 75005 Paris, France*

²*ONERA, The French Aerospace Lab, Base Aérienne 701, 13661 Salon Cedex AIR, France*

**ugo.tricoli@onera.fr*

Abstract: We develop a model of full-field optical coherence tomography (FF-OCT) that includes a description of partial temporal and spatial coherence, together with a mean-field scattering theory going beyond the Born approximation. Based on explicit expressions of the FF-OCT signal, we discuss essential features of FF-OCT imaging, such as the influence of partial coherence on the decay of the signal with depth that is captured by the model. We derive the conditions under which the spatially averaged signal exhibits a pure exponential decay with depth, providing a clear frame for the use of the Beer-Lambert law for quantitative measurements of the extinction length in scattering media.

OCIS codes: 170.4500, 290.4210

1. Introduction

The OCT setup is essentially a low coherence Michelson interferometer, in which one arm collects the light backscattered from the sample, while the other arm produces a reference beam reflected on a mirror [1]. The main feature of an OCT setup is the ability to decouple the depth (longitudinal) and transverse resolutions. Depth resolution is produced by temporal coherence gating, and is controlled by the spectral width of the incident light. Transverse resolution is controlled by the numerical aperture (NA) of the microscope objective in the sample arm [2]. In scanning OCT (S-OCT), a point-by-point image is formed by three-dimensional scanning of a focal spot. OCT systems recording *en face* images in planes perpendicular to the optical axis have also been developed, using spatially coherent illumination as in wide-field OCT (WD-OCT), or spatially incoherent illumination as in full-field OCT (FF-OCT).

Since OCT is expected to collect the singly backscattered photons, the signal is substantially affected by multiple scattering, whose contribution overcomes the signal at depths larger than the scattering mean free path [2].

Despite the success of OCT, from basic to clinical studies, a comprehensive theoretical model of the OCT signal, that handles a description of partial coherence together with a realistic scattering model (beyond the Born approximation), is still missing. In this paper we develop such a model, and use it to discuss different aspects of FF-OCT imaging. We address the question of the decay of the signal with depth, that is captured by a mean-field scattering approach. Depending on the degree of spatial coherence and on the numerical aperture of the illumination/collection optics, we derive the conditions under which the spatially averaged FF-OCT signal exhibits a pure exponential decay with depth. This provides a clear frame for the use of the Beer-Lambert law for quantitative measurements of the extinction length in scattering media.

2. FF-OCT signal

An OCT setup is based on a Michelson interferometer, as represented schematically in Fig. 1. Starting from the source, the beam is divided by a beam-splitter to travel along two arms. The sample arm collects the field backscattered from the sample. In the second arm, a reference beam is produced by reflection on a mirror. The detector collects the intensity resulting from the interference between the sample and reference beams. In FF-OCT, a full-field illumination is used in combination with an array of detectors (in practice a CCD camera) to record the signal at multiple transverse locations in parallel, and produce an *en face* image. This means that both arms contain a microscope objective, not represented in Fig. 1 for simplicity. The state of coherence of the light source plays a crucial role in FF-OCT. Beyond the longitudinal sectioning given by the temporal coherence length (or equivalently the spectral bandwidth), spatial coherence influences

the lateral resolution, as well as the sensitivity to aberrations in the sample arm. In order to understand precisely the role of temporal and spatial coherence, we need to build a model of the FF-OCT signal that includes the scattering model and the main features of the interferometric and broadband detection used in OCT.

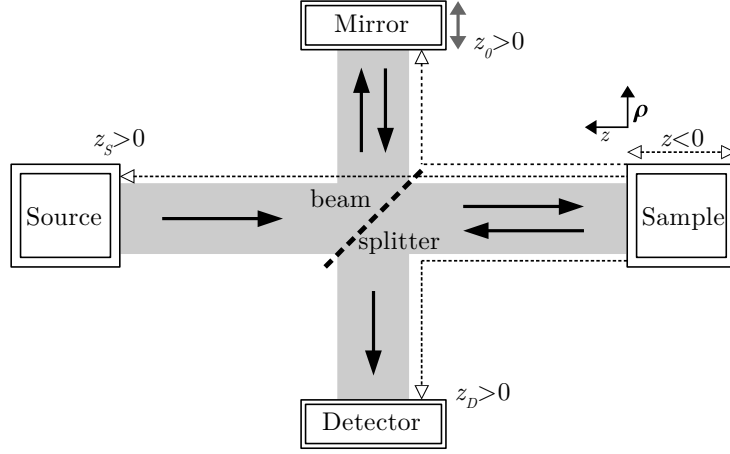


Fig. 1. Schematic view of a FF-OCT setup using a source with partial temporal and spatial coherence. The detector measures the interferogram between the light backscattered from the sample, and the light reflected on the mirror. Illumination and collection optics (microscope objectives) in the different arms of the interferometer are not represented. The z -axis of the reference frame is chosen so that $z = 0$ coincides with the sample plane, with $z < 0$ inside the sample. The source, mirror and detector planes corresponds to $z = z_s$, $z = z_0$ and $z = z_D$, respectively.

Under illumination by statistically stationary light, the intensity recorded by a Michelson interferometer is characterized by three terms: The (time) average intensity of the reference field, the average intensity of the scattered field, and the cross-correlation between them (interference term). Assuming $|E_s| \ll |E_0|$, the signal carrying information on the sample is the interference term (the intensity of the scattered field is negligible, and the intensity of the reference field only contributes as a background signal) [2]. In the frequency domain, the OCT signal measured at a given point \mathbf{r}_D in the detector plane is

$$S(\mathbf{r}_D, \omega) = \overline{E_{\text{ref}}^*(\mathbf{r}_D) E_s(\mathbf{r}_D)}, \quad (1)$$

where E_{ref} and E_s are, respectively, the complex amplitude of the reference and backscattered field at frequency ω , the superscript $*$ denotes the complex conjugate, and the overline means a time averaging over the fluctuations of the partially coherent source.

The incident field E_0 at a point $\mathbf{r} = (\rho, z)$ can be written in the form of a plane-wave expansion

$$E_0(\mathbf{r}) = \int d^2 q e_0(\mathbf{q}) \exp[i\mathbf{q} \cdot \rho - ik_z(q)z], \quad (2)$$

with $k_z(q) = (k_0^2 - q^2)^{1/2}$, the z -axis being taken normal to the sample surface, and following the optical axis in each arm. Assuming a weakly focused beam (the influence the numerical aperture is discussed in section 3), we can perform a zeroth-order paraxial approximation $k_z(q) \simeq k_0$, resulting in $E_0(\mathbf{r}) = E_0(\rho, z = 0) \exp(-ik_0 z)$. The field in the reference arm is assumed to coincide with the incident field longitudinally shifted by the mirror displacement. Under the same paraxial approximation, we can write $E_{\text{ref}}^*(\mathbf{r}_D) = E_0^*(\rho_D, z = 0) \exp[-ik_0(z_D - 2z_0)]$ where z_0 is the position of the mirror. From Eq. (1) and the expressions of E_0 and E_{ref}^* above [1], we can write the FF-OCT signal as

$$S(\mathbf{r}_D, \omega) = \langle S(\mathbf{r}_D, \omega) \rangle + \delta S(\mathbf{r}_D, \omega) \quad (3)$$

with

$$\langle S(\mathbf{r}_D, \omega) \rangle = A \exp[ik_0(2z_0 - z_S - z_D)] \int d^2\rho_S \langle G_R(\mathbf{r}_D, \mathbf{r}_S) \rangle W_0(\rho_S - \rho_D), \quad (4)$$

$$\begin{aligned} \delta S(\mathbf{r}_D, \omega) &= Ak_0^2 \exp[ik_0(2z_0 - z_S - z_D)] \int d^3r' \int d^2\rho_S \langle G_T(\mathbf{r}_D, \mathbf{r}') \rangle \Delta \mathcal{E}(\mathbf{r}') \\ &\quad \times \langle G_T(\mathbf{r}', \mathbf{r}_S) \rangle W_0(\rho_S - \rho_D). \end{aligned} \quad (5)$$

In these expressions we have introduced the cross-spectral density

$$W_0(\rho_S - \rho_D) = \overline{E_0^*(\rho_D, z=0)E_0(\rho_S, z=0)}, \quad (6)$$

that characterizes the state of coherence of the incident field in the sample plane $z=0$. Here we assume that the incoming intensity is uniform over the sample surface, and use a homogeneous Schell model such that W_0 is a function of $\rho_S - \rho_D$ only [2].

It is clear that $\langle S(\mathbf{r}_D, \omega) \rangle$ characterizes the effective medium, and does not carry information on $\Delta \mathcal{E}(\mathbf{r}')$. In order to build the simplest model, we assume weak scattering, meaning that $k_0 \ell_e \gg 1$ with ℓ_e the extinction mean free path characterizing the decay of the average field (the extinction coefficient $\mu_e = 1/\ell_e$ can also be used equivalently). The effective medium, as seen by the average field, is described by a dielectric function $\epsilon_{\text{eff}} = \epsilon_b + i/(k_0 \ell_e)$ (this expression being valid to first order in the small parameter $1/(k_0 \ell_e)$). In this limit, the reflected average Green function $\langle G_R \rangle$ simply describes reflection at the surface of the effective medium, and contributes as a uniform background. Assuming a low index mismatch with $\epsilon_b \simeq 1$, the contribution of $\langle S(\mathbf{r}_D, \omega) \rangle$ becomes negligible. In the following we focus on the contribution $\delta S(\mathbf{r}_D, \omega)$ that carry the relevant information on the image formation process. It is useful to introduce the plane-wave expansion of the average Green function:

$$\langle G_T(\mathbf{r}, \mathbf{r}') \rangle = \frac{i}{2\pi} \int d^2q \frac{g(\mathbf{q})}{k_z(q)} \exp[i\mathbf{q} \cdot (\rho - \rho') + ik_z(q)|z - z'|]. \quad (7)$$

We take $k_z(q) = (k_0^2 - q^2)^{1/2}$ for propagation outside the sample (for $z, z' > 0$), and $k_z(q) = k_z^{\text{eff}}(q) = (\epsilon_{\text{eff}} k_0^2 - q^2)^{1/2}$ for propagation inside the sample (for $z, z' < 0$). The filter $g(\mathbf{q})$ plays the role of a pupil function that limits the transverse wavevector \mathbf{q} within a region bounded by the numerical aperture NA of the objectives (the simplest model for $g(\mathbf{q})$ is a disk with radius $k_0 NA$). For $g(\mathbf{q}) = 1$ (infinite pupil), we recover the Weyl expansion of the free-space Green function. To get an expression of the FF-OCT signal relevant for an analysis in terms of optical transfer function, we insert Eq. (7) into Eq. (5), and perform again a zeroth-order paraxial approximation, using $k_z(q) \simeq k_0$ outside the sample, and $k_z^{\text{eff}}(q) \simeq k_0 + i/(2\ell_e)$ inside the sample. The result is easily written in terms of the 2D Fourier transform of the signal, $\widetilde{\delta S}(\mathbf{q}, \omega) = \int \delta S(\mathbf{r}_D, \omega) \exp(-i\mathbf{q} \cdot \rho_D) d^2\rho_D / 4\pi^2$, and reads

$$\begin{aligned} \widetilde{\delta S}(\mathbf{q}, \omega) &= -4\pi^2 A \int dz' \exp[2ik_0(z_0 - z')] \widetilde{\Delta \mathcal{E}}(\mathbf{q}, z') \exp(-|z'|/\ell_e) \\ &\quad \times \int d^2q' g(\mathbf{q}') g(\mathbf{q} + \mathbf{q}') \widetilde{W}_0(\mathbf{q}'), \end{aligned} \quad (8)$$

where $\widetilde{\Delta \mathcal{E}}(\mathbf{q}, z')$ is the 2D Fourier transform of $\Delta \mathcal{E}(\rho', z')$, and $\widetilde{W}_0(\mathbf{q}')$ is the 2D Fourier transform of $W_0(\rho_S - \rho_D)$. Note that $\widetilde{W}_0(\mathbf{q}') \propto I_0(\mathbf{q}')$, with $I_0(\mathbf{q}')$ the angular distribution of the incident intensity.

A feature of OCT is to integrate the signal over a broad spectral range. For a statistically stationary source, the broadband signal is obtained by integrating the different frequency components over the source bandwidth $\Delta\omega$. Assuming that W_0 and $\Delta \mathcal{E}$ have a weak dependence on ω , the spectral integration gives

$$\int_{\omega_0 - \Delta\omega/2}^{\omega_0 + \Delta\omega/2} \exp[2ik_0(z_0 - z')] d\omega = \exp[2i\bar{k}_0(z_0 - z')] \text{sinc}[(z_0 - z')\Delta\omega/c] \Delta\omega, \quad (9)$$

where $\bar{k}_0 = \omega_0/c$, with ω_0 the central frequency of the source. The sinc function, considered as a function of z' , is centered at z_0 with a width $\ell_\omega = c/\Delta\omega$ corresponding to the temporal coherence length of the incident light, and is responsible for the longitudinal sectioning in OCT. When $\ell_\omega \ll \ell_e$, we can use the approximation $\text{sinc}[(z_0 - z')/\ell_\omega] \simeq \pi \ell_\omega \delta(z_0 - z')$. We

end up with a closed-form expression of the 2D Fourier transform of the broadband OCT signal $\widetilde{\delta S}(\mathbf{q}) = \int_{\Delta\omega} \widetilde{\delta S}(\mathbf{q}, \omega) d\omega$, that depends on the position z_0 of the mirror and on the source bandwidth $\Delta\omega$:

$$\widetilde{\delta S}(\mathbf{q}) = -4\pi^3 A_c \widetilde{\Delta \mathcal{E}}(\mathbf{q}, z_0) \exp(-z_0/\ell_e) \int d^2 q' g(\mathbf{q}') g(\mathbf{q} + \mathbf{q}') \widetilde{W}_0(\mathbf{q}'). \quad (10)$$

Expression (10) of the the FF-OCT signal implicitly involves different length scales, whose interplay is critical in the analysis of the signal: The length scale ℓ_e characterizing the microscopic random inhomogeneities in the sample, the length scale L_e characterizing large-scale deterministic fluctuations of the dielectric function, the temporal coherence length ℓ_ω and the spatial coherence length ℓ_c of the incident light. Expression (10) is similar to that previously derived in Ref. [2]. The main difference is that our derivation includes a scattering model based on a mean-field approach, that goes beyond the Born approximation. An interesting consequence is that the extinction of the signal with depth, due to scattering and absorption, appears explicitly.

3. Depth dependence of the average signal

The decay of the signal with depth is a feature of OCT. For paraxial illumination and detection, and in a medium with $\widetilde{\Delta \mathcal{E}}(\mathbf{q}, z_0)$ independent of z_0 , the signal follows an exponential decay $\exp(-z_0/\ell_e)$, as described by Eq. (10). At higher numerical aperture, a correction to a pure exponential decay is expected, that may also depend on the degree of spatial coherence of the incident field. To address this question, we make use of a second-order paraxial approximation

$$k_z(q) \simeq k_0 - \frac{1}{2} \frac{q^2}{k_0}, \quad (11)$$

$$k_z^{\text{eff}}(q) \simeq \sqrt{\varepsilon_{\text{eff}}} k_0 - \frac{1}{2} \frac{q^2}{\sqrt{\varepsilon_{\text{eff}}} k_0} \simeq k_0 + \frac{i}{2\ell_e} - \frac{1}{2} \frac{q^2}{k_0} + \frac{i q^2}{4k_0^2 \ell_e}, \quad (12)$$

in the plane-wave expansions of the incident field [Eq. (2)] and of the average Green function [Eq. (7)]. Following again the steps leading to Eq. (10), we end up with an expression of the FF-OCT signal that explicitly accounts for the angular aperture of the illumination and detection beams. In order to discuss the depth dependence of the spatially integrated signal, we consider $\widetilde{\delta S}(\mathbf{q} = 0)$, which can be cast in the following form (details of the derivation are given in [1]):

$$\widetilde{\delta S}(\mathbf{q} = 0) = -4\pi^3 A_c \widetilde{\Delta \mathcal{E}}(\mathbf{q} = 0, z_0) \exp(-z_0/\ell_e) \int d^2 q' g^2(\mathbf{q}') \widetilde{W}_0(\mathbf{q}') \exp[-q'^2 z_0 / (2\bar{k}_0^2 \ell_e)]. \quad (13)$$

This expression is well suited to a discussion of the depth dependence of the integrated FF-OCT signal. Note that in practice, an exponential fit to the signal is often used to estimate the extinction mean free path ℓ_e in statistically homogeneous and isotropic scattering media. From Eq. (13), it is clear that at finite NA a deviation from a pure exponential decay may be observed due to the dependence on z_0 of the integral over q' . This integral contains several cutoffs. First, the last exponential term gives a depth-dependent cutoff $q'_{z_0} \simeq \bar{k}_0 (\ell_e/z_0)^{1/2}$. For $z_0 \gg \ell_e$, the integral is restricted to vanishingly small q' , and a pure exponential decay $\exp(-z_0/\ell_e)$ is always expected in the tail of the signal versus depth. Second, the angular spectrum of the Green function $g(\mathbf{q}')$ produces a cutoff $q'_{NA} \simeq \bar{k}_0 NA$, showing that for $NA \rightarrow 0$ a pure exponential decay is observed, in agreement with Eq. (10). Third, the Fourier transform of the cross spectral density $\widetilde{W}_0(\mathbf{q}')$ introduces a cutoff $q'_c \simeq 2\pi/\ell_c$ that depends on the degree of spatial coherence of the incident light in the sample plane. For $\ell_c \rightarrow \infty$ (spatially coherent illumination), a pure exponential decay is also observed. More precisely, to prevent the $\exp[-q'^2 z_0 / (2\bar{k}_0^2 \ell_e)]$ term in the integral to play a role, we need either $NA \ll (\ell_e/z_0)^{1/2}$ (low numerical aperture regime), or $\ell_c \gg \lambda (z_0/\ell_e)^{1/2}$ (coherent illumination).

This qualitative analysis is confirmed by numerical calculations of the spatially integrated signal using Eq. (13), as shown in Fig. 2. A non-exponential decay is observed in the regime $NA \simeq (\ell_e/z_0)^{1/2} \simeq \lambda/\ell_c$. The deviation from a pure exponential decay for $z_0 \lesssim \ell_e$ is enhanced at high NA and low spatial coherence.

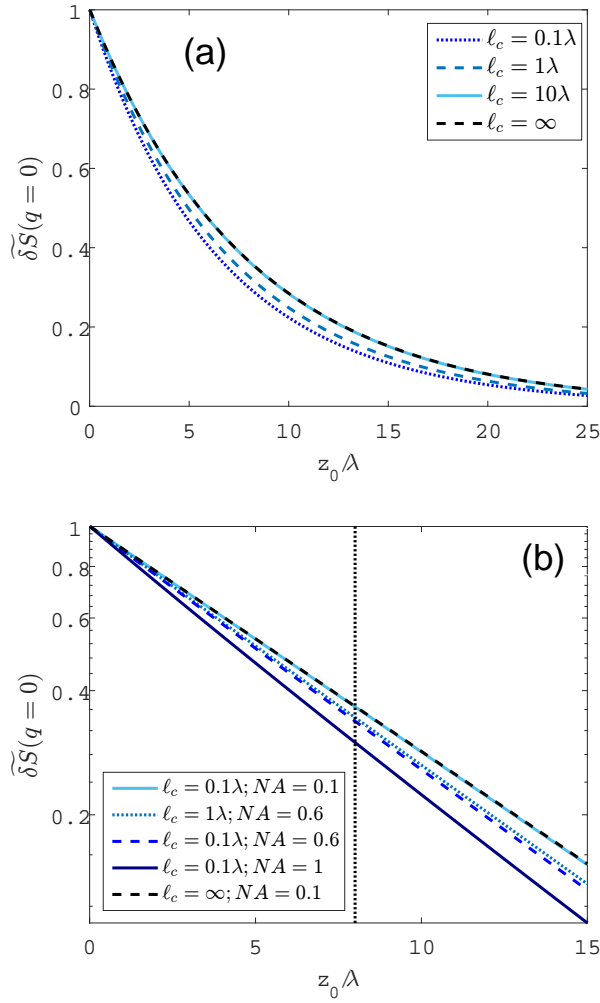


Fig. 2. Spatially integrated FF-OCT signal $\widetilde{\delta S}(\mathbf{q} = 0)$ versus the depth z_0 for different values of the spatial coherence length ℓ_c and numerical apertures NA , normalized by its value at $z_0 = 0$. The central wavelength of the incident light is $\lambda = 800\text{nm}$, the temporal coherence length is $\ell_\omega = 1 \mu\text{m}$, and the extinction length is $\ell_e = 8\lambda$. The pupil function $g(\mathbf{q})$ is modeled by a Gaussian profile $g(\mathbf{q}) \propto \exp[-q^2/(\bar{k}_0 NA)^2]$. The cross-spectral density $\widetilde{W}_0(\mathbf{q})$ in the Gaussian Shell-model is $\widetilde{W}_0(\mathbf{q}) \propto \exp[-q^2 \ell_c^2/(4\pi^2)]$. (a): Signal for different degrees of spatial coherence with $NA = 1$. (b): Signal for different values of ℓ_c and NA . The vertical dashed line corresponds to $z_0 = \ell_e$. Adapted from [1].

4. Conclusions

In summary, we have developed a model of FF-OCT that includes a mean-field scattering theory, in addition to a precise description of temporal and spatial coherence. The model describes the decay of the signal with depth due to scattering and absorption, an essential feature in OCT imaging. It also permits an analysis of the interplay between different length scales characterizing the scattering medium and the degree of coherence of the incident field. Based on explicit expressions of the FF-OCT signal, we have discussed several features of FF-OCT imaging. We have also studied the depth dependence of the signal integrated over the transverse directions, that not only limits the penetration depth in OCT, but is also used to measure the extinction length in scattering materials. For spatially incoherent illumination, and/or with high numerical aperture of the illumination/detection optics, deviations from a pure exponential decay can be observed. A pure exponential decay is always recovered in the tail of the signal versus depth when $z_0 \gg \ell_e$. Our analysis provides a clear frame for the use of the Beer-Lambert law for quantitative measurements of the extinction length in scattering media. The model also provides a framework for a precise analysis of the role of aberrations generated by the optics in the sample arm, or by the scattering medium itself, and for the development of advanced inverse reconstruction procedures going beyond the Born approximation.

References

1. U. Tricoli and Rémi Carminati, J. Opt. Soc. Am. A, **36**, 11, C122-C129 (2019).
2. D. L. Marks, B. J. Davis, S. A. Boppart, and P. S. Carney, J. Opt. Soc. Am. A, **26**, 376-386 (2009).